BOREAS An international journal of Quaternary research

The Lake Paravani archive – a contribution to the late Quaternary landscape evolution of the Lesser Caucasus (Georgia)

DANIEL GADEMANN, NINO USTIASHVILI, LUKA ADIKASHVILI, LEVAN NAVROZASHVILI, NATHANIEL ERB-SATULLO, W. MARIJN VAN DER MEIJ, GIORGI KIRKITADZE, TIIU KOFF, MIKHEIL ELASHVILI, HELMUT BRÜCKNER AND HANNES LAERMANNS

BOREAS

Gademann, D., Ustiashvili, N., Adikashvili, L., Navrozashvili, L., Erb-Satullo, N., van der Meij, W. M., Kirkitadze, G., Koff, T., Elashvili, M., Brückner, H. & Laermanns, H.: The Lake Paravani archive – a contribution to the late Quaternary landscape evolution of the Lesser Caucasus (Georgia). *Boreas*. https://doi.org/10.1111/bor.12669. ISSN 0300-9483.

Lake Paravani, located on the volcanic Javakheti Plateau in the central part of the Lesser Caucasus at 2073 m a.s.l., forms a unique geo-bio-archive for palaeoenvironmental reconstructions in this remote region. Based on sediment cores from the southwestern part of the lake we expand the existing palynological and sedimentological records beyond the Last Glacial Maximum (LGM). For the first time, it is possible to reconstruct the palaeoenvironment in this part of the Lesser Caucasus back to *c.* 28 cal. ka BP. Our study shows that until 16 cal. ka BP glacial conditions dominated (Phase I) in the region; there is, however, proof that the lake already existed during the LGM. In the following transitional Phase II from 16 until 6 cal. ka BP, cold and arid conditions with sparse steppe vegetation and a lowered lake level prevailed. Around 10 cal. ka BP, tree pollen started to expand while herbaceous pollen, especially Chenopodiaceae, declined. In Phase III, since 6 cal. ka BP, mixed forest probably represented the Holocene climatic optimum. Fluctuating lake levels indicate shifting climatic conditions. The minor changes of arboreal pollen hin the uppermost part of Phase II may be an indication of human activity. The more humid, vegetation-rich environment and mild climate around 4.5–2 cal. ka BP correlate with the expansion of the Late Bronze Age settlements in this area (from ~3.5 cal. ka BP/~1.5 ka BC). The proliferation of sites on the plateau, along with even higher-altitude sites possibly dating to the same period, may indicate that this climate amelioration played an important role in enabling more sustained human occupation. The results extend the record on Lake Paravani by several millennia beyond the LGM and complement the palaeo-lake reconstructions of the wider region, e.g. at Lake Van (Türkiye) or Lake Sevan (Armenia).

Daniel Gademann, W. Marijn van der Meij, Helmut Brückner and Hannes Laermanns (corresponding author: h.laermanns@uni-koeln.de), Institute of Geography, University of Cologne, Zülpicher Straße 45, 50937 Köln (Cologne), Germany; Nino Ustiashvili, Luka Adikashvili, Levan Navrozashvili, Giorgi Kirkitadze and Mikheil Elashvili, Cultural Heritage and Environment Research Center, Ilia State University, Cholokashvili 3/5, Tbilisi 0162, Georgia; Nathaniel Erb-Satullo, Cranfield Forensic Institute, Cranfield University, College Road, Cranfield, Bedfordshire, United Kingdom MK43 0AL; Tiiu Koff, Institute of Ecology, Tallinn University, Uus Sadama 5, 10120 Tallinn, Estonia; *received 25th April 2023, accepted 7th June 2024.*

Lakes are dynamic response systems that record ecological, climatic and human-induced changes as well as extreme events in their catchments, thus forming important archives for the Holocene, sometimes even the Pleistocene and beyond (Cohen 2003; Zolitschka *et al.* 2003; Stock *et al.* 2020). The characteristics of their sediments, particulary grain size and geochemical parameters, their floristic and faunistic inventories, are keys to the identification of weathering processes, sediment provenace and human footprint in the lake catchment (Schnurrenberger *et al.* 2003; Dusar *et al.* 2011; Stock *et al.* 2020). It is important to understand the influence of external and internal drivers on sedimentation in interaction with local environmental conditions.

In high mountain lakes conditions are considered to be extreme. Low rock weathering and limited soil development cause highly diluted waters; as a consequence, these lakes are often oligotrophic (Catalan *et al.* 2006). As solar radiation is high at that altitude, much light reaches the lake water during ice-free periods. With their remoteness and small and confined drainage areas, high mountain lakes are very sensitive ecosystems that react directly to environmental change (Catalan *et al.* 2006, 2013; Moser *et al.* 2019).

While there are many lakes in the Lesser Caucasus region, palaeolimnological studies remain sparse, with pollen studies as the only exception. Besides Messager *et al.* (2013, 2021) on Lake Paravani, Connor *et al.* on several smaller lakes from the Javakheti Plateau to the lowlands (Connor *et al.* 2004) and close to Mtskheta (Connor *et al.* 2020) and von Suchodoletz *et al.* (2022), there are no other comparable studies published for the Lesser Caucasus region. The latter publication, focused on a lowland palaeolake in a dry environment (Kakheti, southeastern Georgia), reveals a pattern of accelerating aridification and illustrates regional variability in ecological trajectories. The most adjacent studied major lakes on a wider regional scale are the lakes Van (Wick *et al.* 2003; Stockhecke *et al.* 2014; Simsek & Cagatay 2018) and Hazar (Eris *et al.* 2018; Ön *et al.* 2018) in Türkiye (formerly called Turkey), Lake Sevan in Armenia (Leroyer *et al.* 2016; Robles *et al.* 2022) as well as the lakes Zrebar and Urmia in Iran (Stevens *et al.* 2012) (Fig. 1).

DOI 10.1111/bor.12669

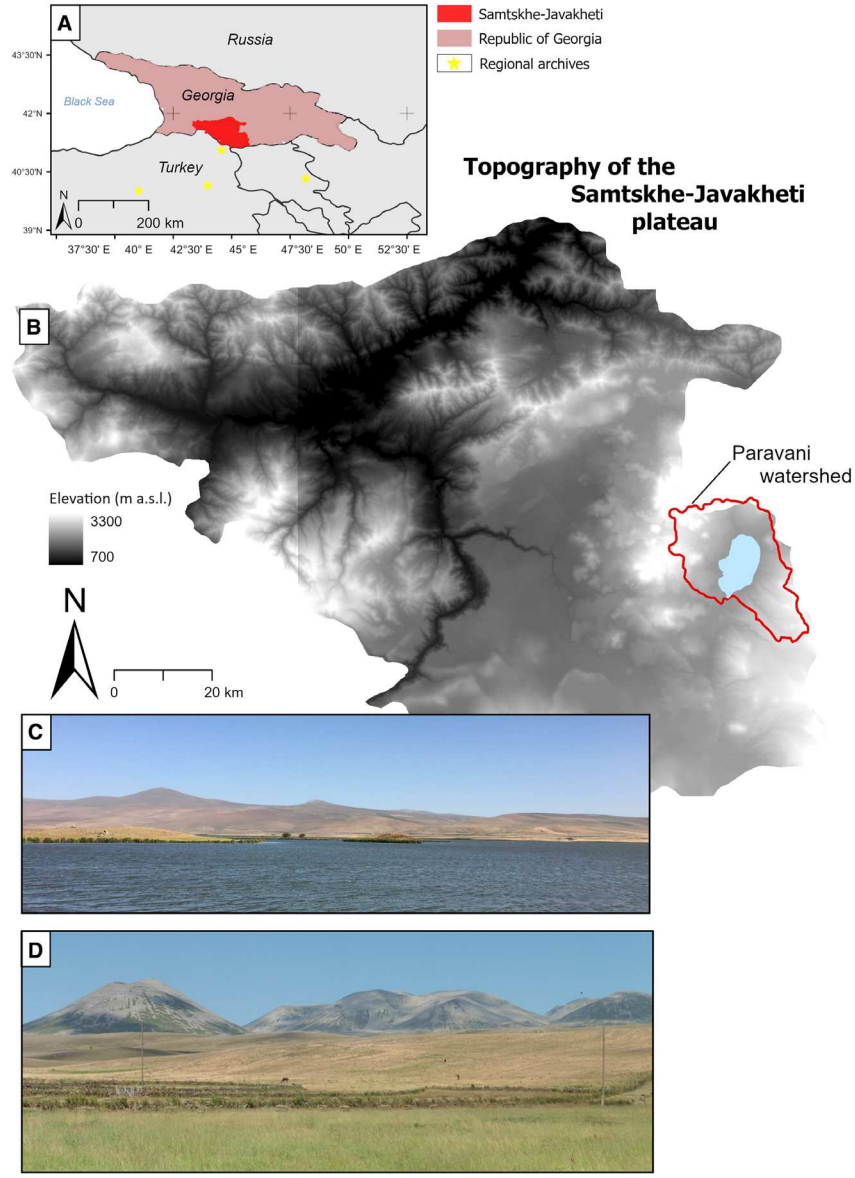

Fig. 1. A. Location of the Samtskhe-Javakheti Plateau within Georgia. B. Topography of the plateau and the Paravani watershed according to Messager *et al.* (2021). C. Lake Paravani, seen from the western shore to the east (photo: H. Brückner, 08/2019). D. Volcanic cones of the Samsari range, western watershed (photo: H. Laermanns, 08/2019).

In the Lesser Caucasus region, the reconstruction of the Holocene environmental evolution has so far focused on the vegetation history of Georgia's Black Sea coast since the Middle Holocene (e.g. Connor *et al.* 2007; de Klerk *et al.* 2009; Shatilova *et al.* 2010), the coastline formation (e.g. Laermanns *et al.* 2018a, 2019) and on river dynamics (von Suchodoletz *et al.* 2015). Several geoarchaeological projects have been carried out concerning the environments of Neolithic and Bronze Age sites, e.g. the anthropologically famous Dmanisi site (Messager *et al.* 2009, 2011), burial mounds on the Bedeni Plateau (Kvavadze *et al.* 2015), as well as settlement mounds on the Colchian plain (Laermanns *et al.* 2018b, 2024) and the lower reaches of the Kura catchment (Hansen *et al.* 2007).

Due to the complex sedimentation pattern in Lake Paravani, it is difficult to assign individual sedimentation processes to the data. Hence, the reconstruction of Messager *et al.* (2013, 2021) is mainly based on a solid pollen analysis, which covers the last 13 millennia. The XRF data provided initial clues to the functioning of the lake system but could not provide more detailed insights into the erosion, transport and deposition processes occurring within the lake and its catchment.

Therefore, based on the analysis of vibrocores from Lake Paravani, our research intends to (i) extend the

existing landscape and vegetation history for the Lesser Caucasus region beyond the Holocene into the Late Pleistocene; and (ii) decipher which internal and external processes and drivers of landscape change played a key role in the formation of the Lake Paravani sediment archive. We use a multi-proxy approach, including XRF-core scanning, grain-size analysis and determination of the carbon content to decipher the depositional environment (facies), weathering regimes, and past lake levels. With pollen analysis, we aim to learn more about the vegetation and its development in the catchment in particular and in the Lesser Caucasus in general.

Study area

Localization and geology

Lake Paravani is located 2073 m above sea level (a.s.l.) on the Javakheti Plateau in the central part of the Lesser Caucasus (Fig. 1), which was formed during the Variscan orogeny by complex folding and overthrusting (Sharkov *et al.* 2015). The plateau, around 2000 m a.s.l., is of volcanic origin and has been forming since approximately 10 Ma in three successive phases of volcanic activity. The Abul-Samsari range, located on the western shore of Lake Paravani, consists of 20 volcanic cones that can be dated to the Middle Pleistocene volcanic activity phase. Dacitic and andesitic rocks are found here (Lebedev *et al.* 2008; Nomade *et al.* 2016; Okrostsvaridze *et al.* 2016). In contrast, the eastern part of the lake catchment consists of basaltic and titanium-rich volcanic rocks from one of the older activity phases (3–1 Ma; Lebedev *et al.* 2008; Lebedev 2015; Nomade *et al.* 2016). Rebai *et al.* (1993) identified numerous faults and folds in the range and throughout the plateau, which are mostly associated with shallow seismic activity. The 1899 and 1986 Paravani earthquakes with magnitudes of 6.1 and 5.6, respectively (Shebalin & Tatevossian 1997; Pasquare *et al.* 2011), and volcanic activity (<13 ka BP) in the northern area of the Abul-Samsari mountain range (Tavkvetili volcano) reflect this high seismic activity of the region (Pasquare *et al.* 2011; Nomade *et al.* 2016). These geological conditions led to the development of many lakes on the plateau, when lava flows and tectonic activity built great depressions, which were then filled with water.

Hydrology

Of these lakes, Lake Paravani is the largest with a surface area of 37.7 km^2, an average depth of approx. 3.1 m and a maximum depth of around 4.35 m (Fig. 2), resulting in a volume of approximately 0.177 km^3 (Japoshvili 2008; Messager *et al.* 2013). The catchment covers 234 km^2 (Messager *et al.* 2021), and a major part of its inflow comes from snow-melt and a number of unknown subaqueous seeps along the western shore (Messager *et al.* 2013) (Fig. S1).

Climate

The supra-regional climate evolution of the plateau is very complex due to its location in the transition zone between the mid-latitude Westerlies and the subtropical High-Pressure System (Joannin *et al.* 2014). The regional climate of the plateau is defined as continental with long, cold winters and short cool summers, with mean annual temperatures around 5.3 °C (Messager *et al.* 2013). Consequently, the lake freezes in the second half of December and usually reaches the thickest ice cover in mid-March; it is ice-free at the beginning of May (Japoshvili 2008). The annual precipitation is 500-600 mm, with the highest amounts in spring and summer and the lowest in January. Within the rough relief many local mountain-valley wind systems arise and cause quick weather changes and frequent thunderstorms, especially in spring (Joannin *et al.* 2014). The average wind speed on the plateau is 5.4 m s^{-1} on an annual average, and on 50% of the days of the year it is 12 m s^{-1} and reaches a maximum of 30 m s^{-1} (Akhalkatsi 2009). Although there are no recent glaciers on the Samsari range, glaciation during the Last Glacial Maximum (LGM) is very likely and supported by supposed Weichselian moraines (Messager *et al.* 2013). Based on the recent local conditions, Dede *et al.* (2017) postulated that large valley glaciers covered the mountain range during that time.

Vegetation

Nowadays, the Javakheti Plateau is almost completely covered by herbaceous vegetation, the most widespread vegetation community being the sub-alpine mountain steppe. Grasses of the Poaceae family, like *Festuca* spp., dominate. Forests are mostly absent; however, archaeobotanical archives suggest that the plateau was more forested until recent times (Arabuli *et al.* 2008; Kvavadze & Kakhiani 2010). Furthermore, two small areas of sub-alpine forest have persisted at the northern ranges of the plateau probably representing remnants of the former forest cover (Connor & Kvavadze 2009; Messager *et al.* 2013).

According to Messager *et al.* (2013), deforestation on the Javakheti Plateau started at 2000–3000 cal. a BP, driven by the slightly drier climate and by human impact. The oldest archaeological sites of the research area date back to the Bronze Age, with the megalithic 'Abuli' complex on the eponymous mountain 2637 m a.s.l. (Jijelava & Simonia 2016). Influenced by these factors, increasing fire frequency had a significant impact on the regional vegetation (Joannin *et al.* 2014). In addition, indicator pollen for human impact, like *Plantago* sp. (grazing) and Cerealia (cultivated taxa), can be traced back for thousands of years (Connor *et al.* 2004).

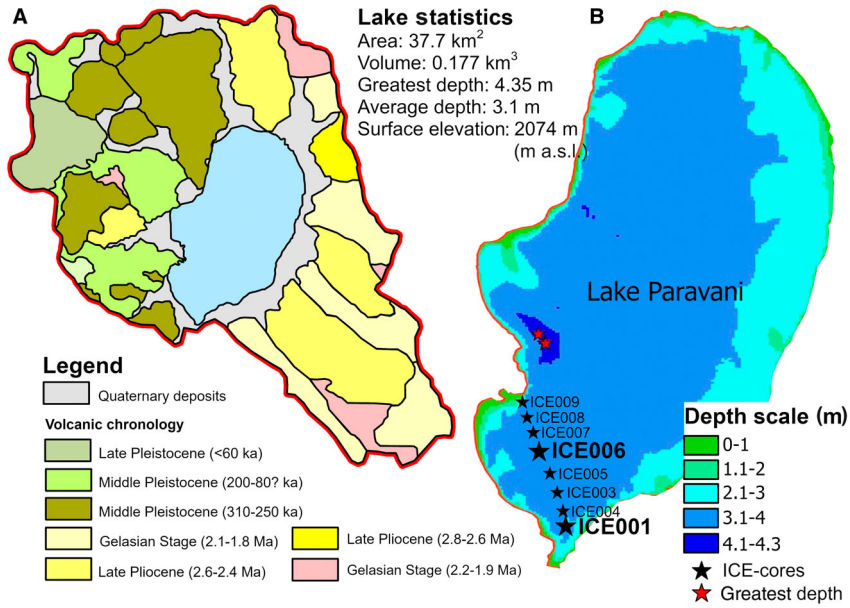

Fig. 2. A. Geological units within the lake watershed modified after Lebedev (2015). B. Bathymetry of Lake Paravani.

Material and methods

Sampling

Fieldwork was carried out between February and March 2019. Eight sediment cores, forming a transect, were drilled in the southern part of the lake from the lake's ice cover, using a Cobra TT (Atlas Copco) percussion corer with closed steel auger heads containing 1-m-long PVC tubes of 5-cm diameter (Fig. S2). ICE001 is located near the southeastern shore of Lake Paravani and represents with a total length of 1.50 m the first core of the transect (Fig. 2B). The core reached a final depth of 190 cm below lake bottom (b.l.b.), but the uppermost 40 cm is missing due to core loss. Cores ICE003 to ICE009 follow in a northwestern direction, all reaching a final depth of about 1 m. With minor variations, all cores were drilled in a water depth of about 3 m (Table 1, Fig. S3).

Laboratory analysis

Sedimentary and geochemical analyses were carried out in the laboratories of the Institute of Geography and the Institute of Geology and Mineralogy at the University of Cologne. After the cores were opened and described, ICE001 and ICE006 were selected for detailed analysis. Despite its less than optimal position at the outflow of the lake and close to the shore, ICE001 was chosen because it is the longest core with a final depth of 190 cm b.l.b., thus probably reaching furthest into the past. In contrast, ICE006 was selected due to its central position and the fine-grained sediment, which, on first inspection after opening, showed homogeneous sedimentation.

Grain-size analysis. – Subsequently, the cores were sampled every 2 cm for sedimentological analysis. These samples were oven-dried at 40 °C and gently crushed with a mortar to break up aggregates. The samples were separated into fine fraction (<2 mm) and coarse fraction (≥2 mm) by sieving. For further analysis, only the fine fraction was used. Hydrogen peroxide (H_2O_2; 15%) and sodium pyrophosphate ($Na_4P_2O_7$; 47 g L^{-1}) were added to remove organic contents and avoid coagulation (Gee & Or 2002). Samples were measured with a laser diffraction particle analyser (Beckman Coulter LS13 320). Each sample was measured three times using the optical Fraunhofer model. Grain-size parameters were calculated

Table 1. Sediment cores from Lake Paravani.

Core ID	Coordinates (X; Y)	Water depth (m)	Core length (cm)	Samples	^{14}C samples
ICE001	41.40445; 43.78924	2.9	150	75	11
ICE003	41.41179; 43.7883	3.3	100	20	–
ICE004	41.40939; 43.788164	3.1	97	48	–
ICE005	41.413637; 43.786151	3.07	98	18	–
ICE006	41.415747; 43.785118	3.1	100	50	5
ICE007	41.417892; 43.784052	3.12	98	50	–
ICE008	41.420076; 43.783042	2.95	100	19	–
ICE009	41.422266; 43.781943	3.0	98	46	–

with GRADISTAT software (Blott & Pye 2001); the nomenclature follows Folk and Ward (1957).

XRF scanning. – First, both split cores were scanned with an Itrax XRF core scanner (Cox Analytical Systems, Mölndal, Sweden) in 1-mm steps using a chrome tube set at 30 kV and 55 mA with a dwell time of 6 s (Croudace *et al.* 2006). In order to flatten the curves, an average from five values was calculated. The values are given in counts per second (cps).

Since the values of the element content are not very meaningful (and are prone to errors such as grain-size effects), we calculated ratios for the purpose of palaeoenvironmental reconstruction. The K/Ti ratio is used as a proxy for physical weathering. Potassium (K) is concentrated in unweathered minerals because it is preferentially leached out of minerals during the weathering process. In contrast, titanium has conservative properties with respect to weathering and transport (Arnaud *et al.* 2012, 2016). Thus, high values of the K/Ti ratio indicate predominantly physical weathering processes in the catchment area of the lake.

With the Ti/Al ratio we tried to distinguish the different source areas of sediments. This is possible because the old basalt and basaltic andesites on the eastern side of the lake are rich in Ti compared to the younger volcanic formations in the catchment. Hence, high Ti/Al ratios suggest a sediment delivery from the eastern side of the catchment (Messager *et al.* 2021).

The Rb/Sr ratio is used as a tracer for chemical weathering intensity, which is a function of temperature and rainfall or moisture. Factors like climate, vegetation cover, the chemical and physical properties of the source rock or enhanced human activity influence the Rb/Sr ratio (Yang *et al.* 2021).

Determination of TOC, C and N. – For additional analyses, the samples were ground using a mixer mill (Retsch MM 400). For the determination of carbon and nitrogen (C; N) as well as the total organic carbon (TOC), the element analyser vario EL cube (Elementar Analysensysteme GmbH, Langenselbold, Germany) was used. 20±5 mg of the ground material from every sample was placed in tin containers (for C, N measurements) and silver containers (for TOC measurement). Before the TOC measurement, the material was treated with hydrochloric acid (HCl, 10%) to dissolve inorganic carbon.

In addition to the TOC value, which provides information on both initial production of biomass and subsequent degree of degradation (integrating the different origins of organic matter, delivery routes, depositional processes, and amount of preservation), the C/N ratio is calculated for the interpretation: values between 4 and 10 indicate fresh organic material from phytoplankton (aquatic), whereas plants on land produce material with C/N ratios of 20 or more (Meyers & Teranes 2002).

Pollen analysis. – From core ICE001, 61 pollen samples were obtained from depths of 41–190 cm b.l.b. and 43 samples from core ICE006. Samples were processed following standard methods (Faegri & Iversen 1989; Moore *et al.* 1991): treatments with HCl and NaOH as well as HF (40 and 60%, respectively), and finally mounting in glycerine. One tablet containing a known number of Lycopodium spores was added to each sample for core ICE001 at the beginning of the treatment, thus enabling the calculation of the total pollen concentration (Stockmarr 1971).

Pollen grains were identified and counted using an Olympus Bx51 microscope equipped with ×10 ocular lens and 40/60 objectives. On average, 300–500 pollen grains of terrestrial taxa were counted for each sample. Due to the low pollen concentration, the pollen sum was close to 100 for the lowermost 65 cm of the core ICE001.

All pollen types were defined according to Reille (1992) and Moore *et al.* (1991). The pollen sum used for percentage calculations was based on the total terrestrial pollen (trees and shrubs [*arboreal* pollen = AP] + upland herbs [*non-arboreal* pollen = NAP]), excluding aquatic vascular plant pollen and spores of mosses and pteridophytes. For non-pollen palynomorphs, the identification of *Pediastrum* algae followed van Geel (2001). Pollen diagrams were created using Tilia software (Grimm 1990). Pollen zones were defined using stratigraphically constrained cluster analysis (CONISS) (Grimm 1987).

Chronostratigraphy. – The chronostratigraphy is based on 16 ^{14}C-AMS ages. ^{14}C-AMS analysis was performed in the Poznan Radiocarbon Laboratory. Since no macro-remains to use Furthermore as dateable material were found in the cores, dating was performed on bulk material. OxCal program v4.4.4 (Bronk Ramsey 2021) and the IntCal20 calibration curve (Reimer *et al.* 2020) were applied to calibrate the radiocarbon ages and to construct an age-depth model. For the deposition model, a P_Sequence was used. This model assumes that the deposition follows a Poisson process, which allows random variations from an average deposition rate (Bronk Ramsey 2008). The level of fluctuation in the deposition process is controlled by a parameter called k. A variable k parameter was chosen to find the best fitting model for our data (Ramsey & Lee 2013). From the modelled age-depth plot, sedimentation rates were calculated by dividing the depth increments between samples by their age differences. Age uncertainties were used to estimate uncertainty in the sedimentation rates. Ages and sedimentation rates are presented with 2-sigma (95.4%) confidence intervals.

Results and facies interpretation

Sediment analysis

Based on the results of the sediment analysis the core ICE001 is subdivided into three sedimentary facies,

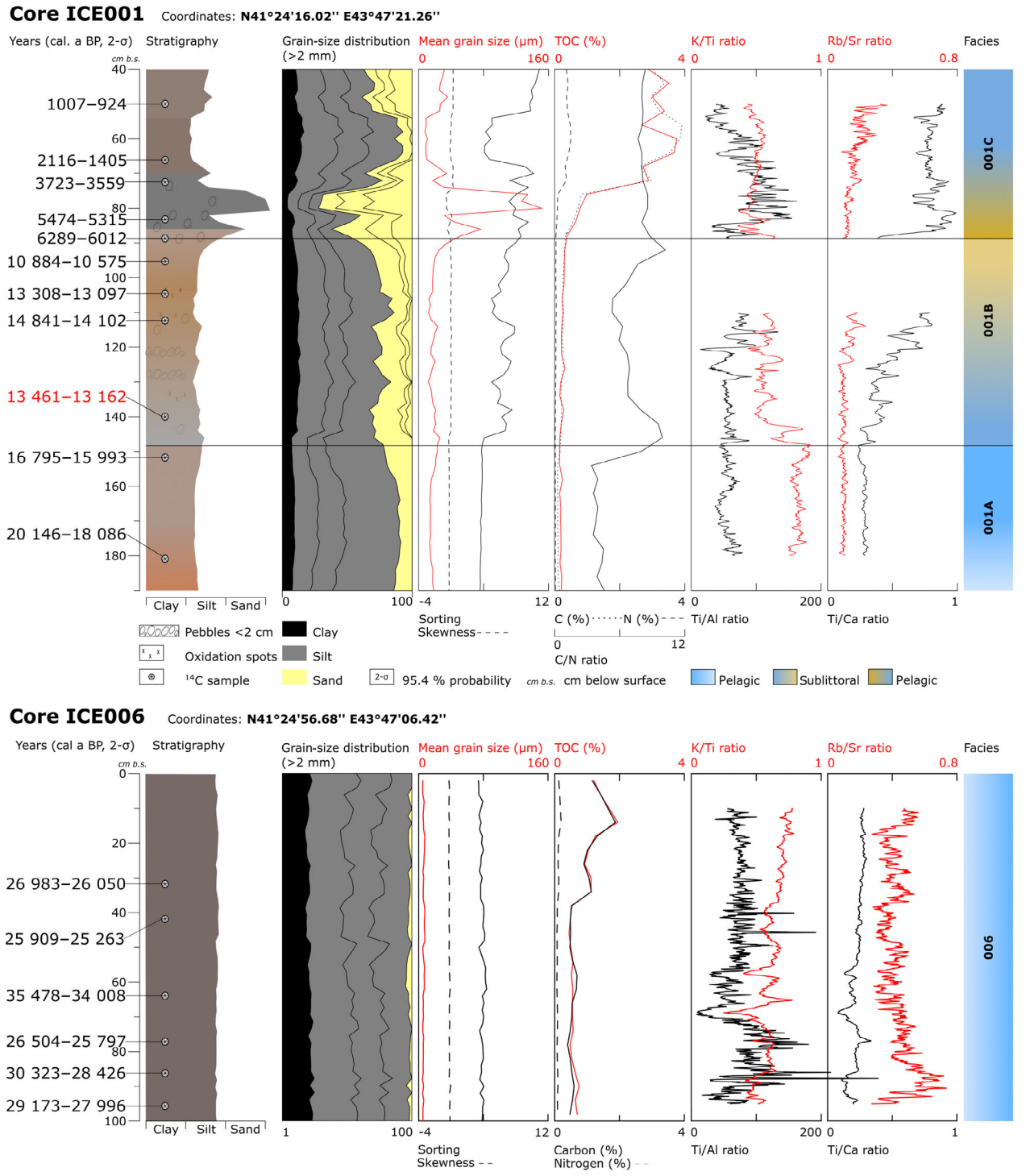

Fig. 3. Sediment cores ICE001 and ICE006 with radiocarbon ages, stratigraphy, granulometry, organic content and geochemistry (from left to right). The age written in red is marked as an outlier.

whereas core ICE006 only represents one sedimentary facies (Fig. 3).

ICE001. – The lowest section from 190 to 148 cm b.l.b., hereafter referred to as facies 001A, is characterized by homogeneous, poorly sorted fine sediment (mean grain size of 13–23 µm with unimodal or bi-modal distributions, Fig. 3) indicating low energy deposition. Within a lake, such sedimentation conditions are expected in the more central, deeper region (pelagic), where the

sediments slowly settle out of suspension (Cohen 2003; Bridge & Demicco 2008). The poor sorting is typical for short transport distances, glacial sediments, and physical weathering (Cohen 2003). Concerning the XRF results, Fig. 3 shows a steady trend for all calculated ratios (K/Ti, Ti/Al, Rb/Sr and Ti/Ca) in the lowermost facies. The low values of Rb/Sr and Ti/Al ratios indicate low chemical weathering and a sediment supply from the western shore of the lake. In contrast, the K/Ti ratio shows high values, which are interpreted as indicative of high physical weathering in the lake catchment (Arnaud *et al*. 2012). The almost complete absence of organic material shows low biological production in the lake, which in turn indicates low temperatures. Also, the C/N ratio is very low.

In contrast, the second facies from 148 to 88 cm b.l.b. (001B) is significantly more heterogeneous and the presence of well-rounded pebbles >2 cm is characteristic (Fig. 3). Between 128 and 120 cm b.l.b., these pebbles occur in larger numbers and are otherwise dispersed in the upper part of the facies within a sandy silt matrix (mean grain size of 12–34 μm, sand accounts up to 39%). These pebbles can most likely be attributed to sublittoral conditions, but may also derive from glacial deposits on the ice sheet and subsequent post thaw deposition on the lake bottom (dropstones; Cohen 2003). Since nearly all pebbles are well rounded, the latter explanation can only be valid for one angular pebble at 148 cm b.l.b., which may represent a dropstone. Changing depositional conditions due to a fluctuation of the lake level, strong currents, shoreface transport and wind influence on sedimentation are characteristic of the sublittoral environment. Consequently, these shallow areas represent only short-term sediment storages and are temporarily affected by erosion (Cohen 2003). The XRF results reflect these depositional conditions, as they show increased variability. Since this core section contains numerous pebbles >2 cm, a strong influence of the grain size on the XRF values is assumed (Rothwell & Croudace 2015). A decreasing trend in K/Ti and an increasing trend in Rb/Sr and Ti/Ca ratios from about 125 cm b.l.b. can be interpreted as increased detrital input and intensification of chemical weathering (Kylander *et al*. 2011; Fritz *et al*. 2018; Yang *et al*. 2021). Relatively stable Ti/Al values suggest that the sediment supply still came from the western shore of the lake. The low TOC content shows no changes as compared to the underlying facies ICE001A; it continues to indicate low productivity in the lake, low allochthonous input and/or poor preservation of organic material (Meyers & Teranes 2002). However, the C/N ratio rises compared to ICE001A.

The uppermost facies (88–40 cm b.l.b., 001C) is clearly separated from the underlying sediments by a 20-cm-thick layer of well-rounded pebbles >2 cm in a coarse sediment matrix (mean grain size up to 150 μm; Fig. 3). A shift of the facies from the sublittoral to the beach seems to be the most likely interpretation. It is supported by the fact that the samples show a high similarity to the recent beach in terms of mean grain size and sorting (Cohen 2003). Thus, this layer represents a good lake level indicator. From 88 cm b.l.b. onwards, the XRF plots of all element ratios reveal a steady decrease towards the top (Fig. 3). K/Ti ratios show the lowest values of the whole core and indicate lower rates of physical weathering (Arnaud *et al*. 2012) while elevated Rb/Sr ratios display increased chemical weathering (Yang *et al*. 2021). The relatively high values of Ti/Al ratios compared to the facies 001A and 001B indicate a shift of the supply area of sediments to the eastern shore of Lake Paravani (Messager *et al*. 2021). The rising trend of organic carbon indicates a significant increase in organic production in the lake and the C/N ratio of about 8 suggests an aquatic origin of the organic material (Meyers & Teranes 2002). A lower detrital input in relation to the other two facies is interpreted based on the greater C/N ratio (Messager *et al*. 2021).

ICE006. – Due to the homogeneous grain-size distribution (unimodal or bi-modal for all samples), the absence of any sedimentary structures and only minor changes in the geochemical parameters, drill-core ICE006 is not subdivided into individual facies (Fig. 3). Rather, facies 006 represents one depositional environment. The very fine-grained sediments with an average grain size between 4.8 and 7.8 μm (sand fraction absent or <5%, silt fraction up to 80%) indicate a depositional environment similar to facies 001A, without a significant influence of a current. The calculated element ratios are partly contradictory to the results of ICE001, especially the Rb/Sr ratio. The latter is characterized by large variations in the range of 0.1–0.7 and therefore not comparable to facies 001A. The K/Ti ratio shows an increasing trend to the top of the core with some positive and negative peaks around 60 cm b.l.b. A prominent Ti/Al peak at 82 cm b.l.b. is very striking, since otherwise this ratio is characterized by lower values. For most sections of ICE006 a sediment supply from the western shore is indicated. The low and constant values of the Ti/Ca ratio point to low detrital input throughout the core. Regarding the TOC content, Fig. 3 shows a clear bisection of the core ICE006: the lower unit between 100 and 38 cm b.l.b. displays low values of TOC (0.42–0.73%), whereas the part from 38 cm b.l.b. onwards shows an increasing trend with the highest value of 1.87% at 14 cm b.l.b.

Pollen analysis

Results of pollen analysis for ICE001 and ICE006 are presented in the pollen diagram (Fig. 4). Using the CONISS method the pollen diagram of ICE001 can be divided into three zones that nearly match the sedimentary facies. As more sedimentological data are available,

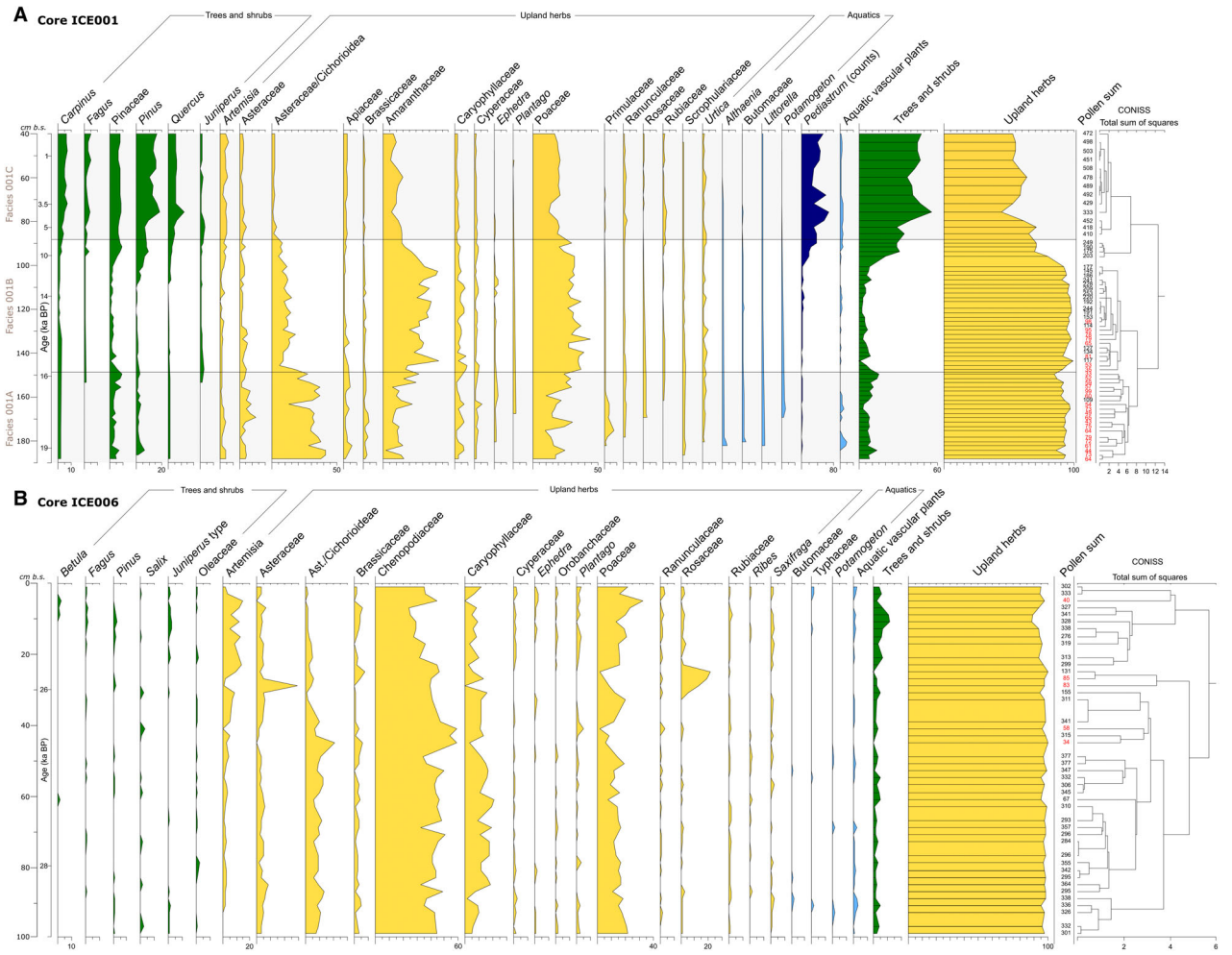

Fig. 4. A. Pollen diagram of core ICE001. B. Pollen diagram of core ICE006 (only selected species are shown). Pollen concentrations below 100 counted preserved pollen per sample are marked in red.

the sedimentological facies are used for interpretation. Results of pollen analysis for ICE006 also match the classification into only one facies. The total pollen concentration of ICE001 shows fewer than 100 grains per 1 g of dry sediment in the lower part (190–150 cm), a slight increase from 150 cm onwards and maximum values in the uppermost part (starting from 90 cm).

ICE001. – In the first pollen zone (190–148 cm b.l.b., marked in grey in Fig. 4), the pollen concentration is very low and should be interpreted with great caution. Herbaceous taxa like Poaceae, Asteraceae/Cichorioideae and Chenopodiaceae are abundant. NAP values vary between 86 and 97%, thus significantly defining the pollen assemblage. Despite tree pollen making up 3–14% in this zone, this pollen spectrum is characteristic of an open vegetation cover, typical of steppe environments. An open vegetation cover of the landscape is supported by the occurrence of *Ephedra* pollen in all samples of this zone. The low pollen concentration and steppe vegetation coincide with the presumed cold climatic conditions that prevailed during the end of the LGM. Since pollen produced by aquatic plants (Alismataceae, Butomateae families and the genera *Althaenia*, *Lemna*, *Littorella*, *Tipha*) also occurs up to 5%, we assume that a lake existed at this time. The low C/N ratios confirm aquatic plant production and therefore indirectly low terrestrial plant production (Meyers & Teranes 2002). The extremely low concentration might reflect the glacial conditions and therefore very sparse vegetation during the time of their deposition.

The second pollen zone (148–100 cm b.l.b.) does not exactly fit the existing facies classification, as the upper facies boundary differs by 12 cm downwards (since there is a very prominent change in the pollen assemblage). A marked decrease in Asteraceae/Cichorioideae and an increase in Chenopodiaceae pollen at the beginning of this zone (around 148 cm b.l.b.) are striking. The pollen of Poaceae is still present in high values (up to 40%). AP further decreases (<10%) and is only present

sporadically, while NAP ranges between 80 and 99% with a gradual decrease and the lowest value at the end of this zone. Pollen of aquatic plants is very sparse in this zone, which is also reflected in the increasing C/N ratios (Meyers & Teranes 2002).

The last pollen zone (100–40 cm b.l.b.) is characterized by a sharp increase of arboreal pollen taxa, both for conifers such as *Pinus*, Pinaceae and deciduous trees like *Betula* and *Carpinus*. Due to the poor state of preservation, the *Quercus* pollen could not be differentiated between *Q. ilex*-type (evergreen) and *Q. pubescens*-type (deciduous). This increase in AP with a peak at 77 cm b.l.b. (53%) clearly shows the forest expansion in this region during that time. Additionally, *Ephedra* pollen are not recorded in this zone; their absence supports the interpretation of a warmer climate and probably more forested landscape (Kaplan 2013). It is interesting to note that the counts of algae *Pediastrum* increase significantly from 100 cm b.l.b. onwards and match the AP peak at 77 cm b.l.b. Since no regression of AP taxa can be found towards the upper end of core ICE001, a human-induced deforestation of the plateau is not recorded.

ICE006. – The pollen diagram of core ICE006 is characterized by the prevalence of NAP (non-arboreal pollen/upland herbs) for the entire sediment sequence (NAP values between 89 and 100%). Therefore, it was not possible to separate any pollen zones in this core. Chenopodiaceae (24–59%), Caryophyllaceae (0–20%), Poaceae (2–32%) and *Artemisia* (1–15%) are the dominant taxa, with Chenopodiaceae prevailing amongst them. From the abundant occurrence of these taxa, it can be assumed that open, steppe and semi-desert vegetation dominated the landscape (Cromartie *et al*. 2020). It is interesting to note that this pollen assemblage closely resembles the first zone of core ICE001. Although the taxon *Ephedra* occurs only sporadically, the interpretation of a steppe environment fits well. Furthermore, the presence of pollen of aquatic vascular plants (Alismataceae, Butomateae families and the genera *Althaenia*, *Lemna*, *Littorella*, *Tipha*) throughout the core suggests the existence of Lake Paravani in the Late Pleistocene.

Compared to core ICE001the pollen preservation in ICE006 is significantly better, which can be attributed to sediment properties. This is surprising especially compared to the lowermost pollen zone of core ICE001.

Chronology

Core ICE001 covers ages that range from the Late Pleistocene (~20 cal. ka BP) to the Late Holocene (~970 cal. a BP). In contrast, core ICE006 exhibits only Pleistocene ages (~28–26 cal. ka BP; cf. Table 2). Figure 3 shows the modelled age-depth plot of core ICE001. Most of the ages show a clear increase with depth. The model identified sample ICE001-6 as an outlier, as its age does not fit the age-depth trend; thus, it was left out of the further analysis. The calibrated radiocarbon ages in the core barely overlap with their uncertainties, leaving the modelled ages to be very similar to the calibrated radiocarbon ages. Since for all radiocarbon ages (16) bulk sediment was used, the carbon contents are very low and the chronology should be treated with caution. Bulk material, which may be used for ^{14}C dating in the absence of directly determinable organic matter, is prone to error and the assignment of the sediment deposition time is not certain (Vogel *et al*. 1989). Following Björck and Wohlfarth (2001) this holds especially true for sediments with low carbon contents (<2%), a phenomenon that is frequently observed in Lateglacial sediments.

Furthermore, in the (peri-)glacial limnological context of the Late Pleistocene, it seems possible that Lake Paravani was cut off from exchange with the atmosphere by ice cover for an extended period, and thus the original ^{14}C/^{13}C ratio is depleted. This effect can also be observed when the lake was fed mainly by meltwater from glaciers (Björck & Wohlfarth 2001).

The allochthonous organic carbon source is problematic, since we cannot exclude (i) a prolonged ice cover and therefore a prolonged time period before the plant material from the catchment was deposited into the lake and (ii) that the allochthonous organic carbon matter consists of soil organic matter (SOM), which may represent very old carbon (especially true for cold environments) (Strunk *et al*. 2020). The sedimentation rates ranged between 2×10^{-3} and 2×10^{-2} cm per year, with the highest rates at the end of the LGM and in the last ~2000 years. Considering the autochthonous organic carbon in the bulk samples: as there is no limestone in the catchment of the lake, the dissolved bicarbonate (which is the main carbon source for all diatoms, algae and lacustrine plants) reflects the contemporaneous atmospheric ^{14}C concentration, thus, a legacy from the watershed can be excluded (Strunk *et al*. 2020).

Despite the mentioned uncertainties, the general chronology for ICE001 should be accepted as given because firstly the chronology is consistent in itself, secondly it is supported by the sedimentological and pollen data, and thirdly the mentioned sources of potential errors indicate a glacial context that prevailed during the dated time-span.

Furthermore, the large time-span recorded by the only 150-cm-long sediment succession ICE001 implies a high potential for a hiatus (Messager *et al*. 2013). The transitions between the facies, where the sedimentation conditions change, are of particular interest. Especially around the palaeo-beach layer (88–68 cm b.l.b.) hiatuses (H1, H2; Fig. 5) are very likely, since erosion or no sedimentation during emerging phases are phenomena associated with beach formation. In the age-depth model in Fig. 5, these areas display the lowest sedimentation rates. Around 140 cm b.l.b. another hiatus (H3, Fig. 5) seems very likely, since an inversion of radiocarbon dates

Table 2. ^{14}C data sheet. Calibration with Calib 8.2 (Stuiver *et al.* 2021) using the IntCal20 calibration curve (Reimer *et al.* 2020). Lab. code: Poznan Radiocarbon Laboratory (https://radiocarbon.pl/en/ams-laboratory/), SD = standard deviation; b.l.b. = below lake bottom.

^{14}C-AMS Lab. ID	Sample ID	Depth (cm b.l.b.)	^{14}C age (a BP)	SD (±)	δ^{13}C (AMS) (‰)	Age (2σ) (cal. a BP)	Median age (cal. a BP)
Poz-172965	ICE001_050	50	1070	30	−23.5	1007–924	970
Poz-129699	ICE001_066.5	66.5	1835	30	−31.6	2116–1405	1753
Poz-172966	ICE001_072	72	3400	35	−23.9	3723–3559	3637
Poz-172956	ICE001_083.5	83.5	4670	35	−24.3	5474–5315	5398
Poz-159887	ICE001_088	88	5395	35	−25.1	6289–6012	6216
Poz-173051	ICE001_093.5	95.5	9490	60	−28.0	10 884–10 575	10 767
Poz-173049	ICE001_104.5	104.5	11 300	70	−28.8	13 308–13 097	13 198
Poz-159888	ICE001_112	112	12 350	60	−28.5	14 841–14 102	14 407
Poz-159889	ICE001_140	140	11 420	80	−29.6	13 461–13 162	13 293
Poz-129700	ICE001_152.5	152.5	13 560	120	−35.4	16 795–15 993	16 373
Poz-129702	ICE001_181.5	181.5	15 630	450	−42.1	20 146–18 086	18 987
Poz-129557	ICE006_032.5	32.5	22 240	150	−27.7	26 983–26 050	26 574
Poz-129558	ICE006_042.5	42.5	21 300	160	−32.6	25 909–25 263	25 639
Poz-129559	ICE006_064.5	64.5	30 220	400	−29.9	35 478–34 008	34 743
Poz-129560	ICE006_077.5	77.5	21 890	210	−28.3	26 504–25 797	26 166
Poz-129561	ICE006_086.5	86.5	24 780	290	−33.5	30 323–28 426	29 027
Poz-129562	ICE006_095.5	95.5	24 450	250	−35.7	29 173–27 996	28 674

occurs and pebbles <2 cm, which may represent fluvial deposition (associated with erosion), occur. All in all, the interpretation of sublittoral conditions with changing deposition patterns suggests a hiatus.

For ICE006 the chronological classification into the Late Pleistocene has to be treated with even greater caution. Since we assume redeposition and deformation by glacial or glacifluvial processes (detailed discussion in the next chapter), we did not create an age-depth model.

Correlation of the cores

The presented facies classification as well as the dating results, confirm the hypothesis of Messager *et al.* (2021) that the depositions within Lake Paravani yield rather complex records. The recent position of the individual cores in the lake cannot adequately explain the highlighted differences between them. While the near-shore position of core ICE001 in the flow area upstream of the recent Lake Paravani outflow is surely responsible for some differences in terms of depositional patterns, it does not provide an explanation for the chronological differences. In this context, Messager *et al.* (2021) suggested effects of earthquakes as a possible explanation for the complex palaeoecological records, since the lake is located in a seismically active area (Rebai *et al.* 1993; Shebalin & Tatevossian 1997; Pasquare *et al.* 2011). The discrepancies between the two cores could also be resolved with an aeolian redistribution of sediments due to katabatic winds during the Late Pleistocene (Nutz *et al.* 2018; Messager *et al.* 2021). Furthermore, a lava flow from the Abul–Samsari mountain range flowing into the lake can be excluded, since no lava flow has reached the shores of Lake Paravani since 30 cal. ka BP (Geological Map, Lebedev 2015).

With respect to the cores presented here, the assumption that the sediment succession ICE006 was redeposited by glacial or glacifluvial processes fits best. The fine-grained, glacially deposited sediments of the core were pushed together by a mass movement originating from the western shore of the lake. There, satellite images, field observation and research reveal relict moraines all over the Abul–Samsari mountain range down to the shores of Lake Paravani. (Guillou *et al.* 2004; Nomade *et al.* 2005; Messager *et al.* 2013) and therefore a high potential glacial and glacifluvial dynamic during the LGM and the subsequent Pleistocene–Holocene transition. The geological footprint of this mass movement is clearly visible as slump and slide structures on the bathymetric map in Fig. 1 (lower left corner). A lobe-shaped structure is located directly west of the location of ICE006 (Fig. 1). Since the distance to the slopes and the fine-grained homogeneous sediments in ICE006 contradict direct glacial origin, we rather assume glacifluvial origin.

Even if we acknowledge the chronostratigraphy of ICE006 as disturbed due to redeposition, its sparse vegetation indicated by the pollen diagram resembles closely the lowermost part of ICE001, and therefore gives information on the Late Pleistocene. Although there remain some uncertainties associated with the deposition of the material and the erosion of the Holocene top layers both cores provide an overview of the landscape evolution over the last 28 000 years.

Palaeoenvironmental and palaeoecological evolution

Glacial phase in the Late Pleistocene (approx. 28–16 cal. ka BP). – This phase of the lake evolution is represented by facies 001A and 006. Both facies represent pelagic depositional conditions. Thus, higher lake levels are

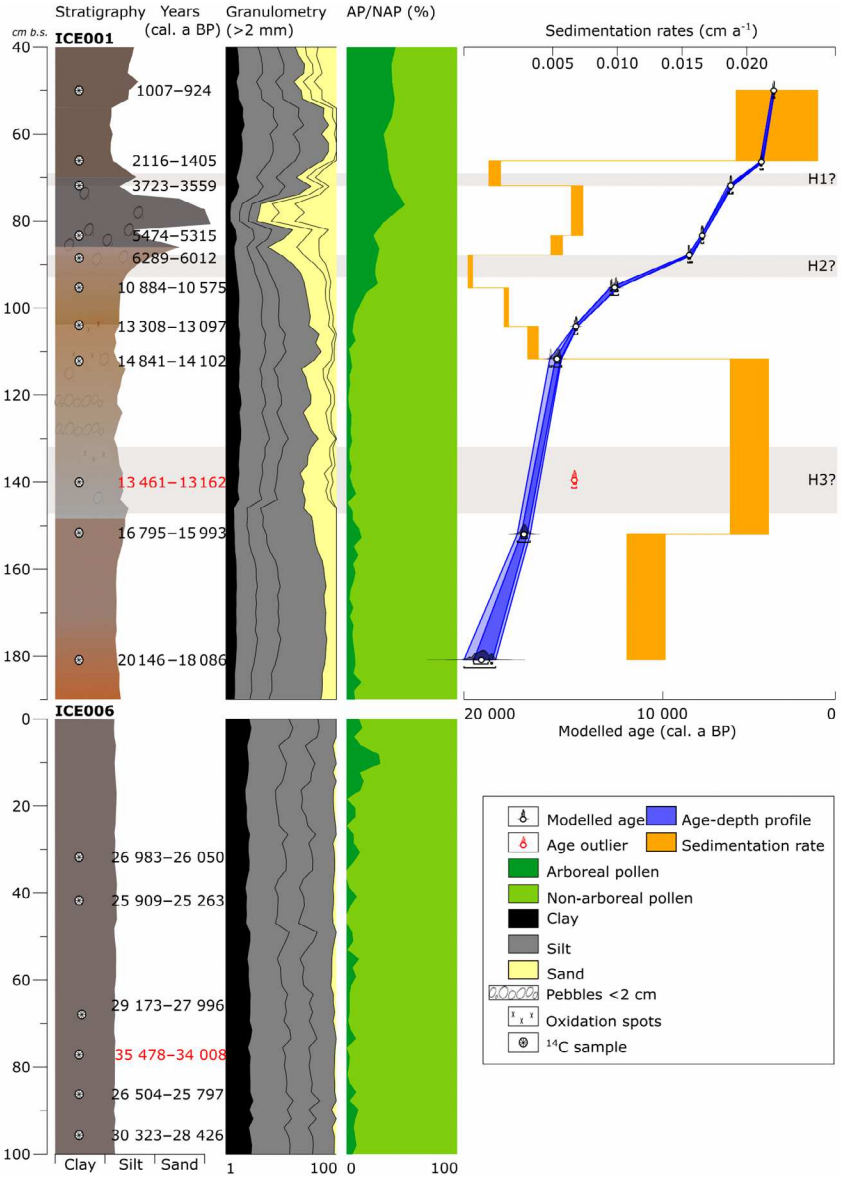

Fig. 5. Synopsis of sediment cores ICE001 and ICE006 with age-depth model and sedimentation rates. Ages and rates are presented with 2-sigma confidence intervals. The outlier ICE001_6 is indicated in red. Grey horizontal bands indicate three possible hiatuses in the stratigraphical record.

inferred. Following Stockhecke *et al.* (2014), the three water balance variables precipitation, runoff and evaporation are the long-term drivers of lake level changes and, thus, an indirect climate proxy. Higher lake levels (or similar to the recent one) therefore imply humid and cold conditions before and during the LGM. The absence of organic material in both facies indicates a low productivity in the lake, which confirms low temperatures and prolonged ice cover with low nutrient input into the lake (Meyers & Teranes 2002; Kleeberg *et al.* 2010). Low allochthonous input of organic material from the catchment can also be considered, indicating poorly developed soils (Messager *et al.* 2013; Cagatay *et al.* 2014). The extremely low pollen concentration in both facies supports the interpretation of a sparse vegetation cover. Herbaceous species such as Asteraceae, Chenopodiaceae and Poaceae are dominant and very typical of (peri-)glacial phases (Messager *et al.* 2021). Particularly in core ICE006, the glacial conditions become obvious, as Chenopodiaceae are predominant and hardly any tree pollen are found (which might have been transported over larger distances by wind). Since aquatic taxa such as Althaenia, Littorella and Butomaceae occur in both facies, Lake Paravani must have existed during that time.

Glaciers may have acted as drivers of physical weathering providing fine-grained sediments in large quantities by abrasion of the bedrock in the Abul-Samsari

mountain range, which is shown by the prominent occurrence of silt and by high values of K/Ti in facies 001A (Arnaud *et al*. 2012). In the glacial context, fluvial transport by meltwater and aeolian transport (due to the lack of vegetation cover) of the fine material is common, wherefore a lot of material could be transported into the lake, resulting in high sedimentation rates (Leemann & Niessen 1994). According to the ^{14}C age estimate (ICE001_2 bulk) at 152.5 cm b.l.b., these conditions prevailed until *c*. 16 400 cal. a BP.

Transition phase from Late Pleistocene to Middle Holocene (approx. 16–6 cal. ka BP). – The transition from facies 001A to facies 001B implies a shift in conditions from the pelagic to the sublittoral zone at the coring site, as the deposition energy increases (Cohen 2003). An increase in aridity is probably the cause of the lowering of the lake level, which is associated with this transition (Wick *et al*. 2003). K/Ti values decrease from the facies boundary at 148 cm b.l.b., suggesting a decrease in physical weathering. The detrital input remains high, as high values of Ti and Fe indicate. The sharp decrease of Asteraceae/Cichorioideae pollen on the one hand and the increase of Chenopodiaceae pollen around 148 cm b.l.b. on the other hand support the interpretation of an increasing aridization of the climate. The occurrence of well-rounded pebbles >2 cm in a fine-grained sediment matrix between 128 and 120 cm b.l.b. indicates a fundamental shift of the depositional conditions with increasing aridization. Most likely, the drilling site was under fluvial influence after the water level was lowered significantly, thus becoming part of the channel flowing out from the lake. An exact chronological classification of the (partial) drying up of the lake at this site is difficult, but the ages at depths of 140 and 112 cm b.l.b. – ranging from 14 841 to 13 162 cal. a BP – give an approximate time period during the 15th–14th millennium BP. A hiatus (H3) in this range of the sediment succession seems very likely since fluvial influence and deposition are usually associated with erosion. Overall, the transition from glacial to interglacial conditions at drill site ICE001 is associated with frequent changes in depositional environments (facies) and incomplete preservation of sediments due to erosion.

In the pollen diagram, a hiatus (H3) is not directly visible, but the pollen in this facies are poorly preserved. After the significant shift at the beginning of the facies, especially in terms of herbaceous species, the pollen composition remains relatively stable until about 100 cm b.l.b. Tree pollen are very rare (even lower than in facies 001A) while Chenopodiaceae as well as Poaceae are predominant. Following 100 cm b.l.b., a sharp increase in arboreal pollen is significant, probably representing the tree expansion on the Javakheti Plateau after the LGM. Especially coniferous taxa such as Pinaceae lead to an increase in arboreal pollen. Deciduous species like *Carpinus* spp. and *Quercus* spp. increase only slightly and may reflect tree expansion on the regional scale. According to the age-depth model, the tree expansion on the plateau started at around 8 cal. ka BP. This is accompanied by a marked decline in herbaceous pollen; especially a sharp decline of Chenopodiaceae is evident.

The absence of organic material throughout the facies further indicates low productivity in the lake and still cold prevailing temperatures. While the pollen record may reflect the climatic evolution with a certain delay due to individual dispersal of species (Messager *et al*. 2021), the sedimentological changes are representative for local aspects and more accurate concerning the chronology.

Middle to Late Holocene evolution (approx. 6–1 cal. ka BP). – Facies 001C, representing the evolution of the lake since the late 7th millennium BP (ICE001_4 bulk; 88 cm b.l.b.), is clearly separated by a palaeo-beach layer (88–68 cm b.l.b.) from the facies below. The lakeshore must have shifted by at least 250 m, as compared to the present distance of the drilling site from the southwestern shore. The age (ICE001_1 bulk; 66.5 cm b.l.b.) just above the palaeo-beach layer, which is a good lake level indicator, dates to 2116–1405 cal. a BP. The ages within the palaeo-beach layer, 5474–5315 cal. a BP (83.5 cm b.l.b.) and 3723–3559 cal. a BP (72.5 cm b.l.b.), clarify that the lower lake level persisted for several millennia during the Middle Holocene (Atlantic and Subboreal periods).

After the deposition of the palaeo-beach layer (and the hiatus H1), a rising lake level can be inferred in comparison to facies 001B, which suggests a positive water balance. As there were no more glaciers on the plateau during that time, the positive water balance must have resulted from increased precipitation. It is very likely that the climate was becoming more humid. The initially slow (88–76 cm b.l.b.) and then sudden increase in organic carbon content at 72 cm b.l.b. points to higher productivity in the lake and rising temperatures from about 6 cal. ka BP onwards (Meyers & Teranes 2002). Additionally, a higher organic input from the catchment area, indicating an expansion of the vegetation cover, is evident, which fits well with the pollen diagram.

After the reforestation started around 100 cm b.l.b. in facies 001B, the share of arboreal pollen reaches its peak at 77 cm b.l.b. The occurrence of species like *Pinus*, *Quercus* and *Carpinus* indicates an expansion of a mixed forest in the catchment area of the lake after 6 cal. ka BP, probably representing the Holocene climatic optimum. The minor changes of arboreal pollen in the uppermost part of the facies (50–40 cm b.l.b.) might be explained by shifting climatic conditions after the Holocene climate optimum, but could also hint at human presence at least since the Bronze Age (Joannin *et al*. 2014; Jijelava & Simonia 2016; Narimanishvili 2019). However, Messager *et al*. (2021) state that, even though the archaeological settlements or burial mounds are of Bronze Age origin,

the evidence of human activity is rather muted before about 2 cal. ka BP.

The K/Ti ratio mirrors these changes, since low values in facies 001A point to a change in the weathering regime. Due to the higher temperatures and more rainfall, chemical weathering outweighs physical weathering. Higher values of Ti/Al indicate a shift in the sediment delivery regime. In facies 001A and 001B, the lower ratios imply delivery of sediments from the western shore, whereas the high values in these facies indicate delivery from the catchment east of the lake (Messager *et al*. 2021).

Due to the loss of the uppermost 40 cm b.l.b. of the core, we are unfortunately unable to make any conclusions about the development of the lake over the last thousand years. However, the age at 50 cm b.l.b. (1007–924 cal. a BP) suggests increased sedimentation rates, since the uppermost 50 cm of the sediment must have stored the last thousand years with estimated average sedimentation rates of 0.05 mm per year.

Lake Paravani and its significance for the palaeoenvironmental reconstruction of the high mountain areas of the Lesser Caucasus

Compared to Messager *et al*. (2013, 2021), the analysed cores ICE001 and ICE006 cover a considerably longer time-span. The lithological characteristics between the cores differ significantly from cores PAR-09-01 and PAR-12-04 for several reasons. For ICE001, the older ages can be explained by the greater final drilling depth of 190 cm b.l.b., and the lithological differences fit with the complex depositional patterns already detected by Messager *et al*. (2021) and result above all from the different positions within the lake. Core ICE006 takes a special role, due to the assumed glacifluvial redeposition.

The interpretation of facies 001A and 006 as glacial deposits at a higher (or equal to) lake level than today before and during the LGM (about 20 cal. ka BP) is consistent with findings from other lakes in the region. Sockhecke *et al*. (2014) and others (Landmann *et al*. 1996; Cagatay *et al*. 2014) identified higher lake levels at Lake Van (eastern Anatolia, Türkiye) during the LGM. The authors associated the lake level highs with a grey, homogeneous, fine-grained facies without organics. It is comparable to facies 001A and 006, and strengthens our interpretation (Cagatay *et al*. 2014; Stockhecke *et al*. 2014). Possible explanations for higher lake levels during the LGM were also offered by Ön *et al*. (2018) at Lake Hazar, central Anatolia, Türkiye. Due to the by-then minimal differences between summer and winter solar irradiation, the seasonality of the climate was weakened. The reduced evaporation caused by cold, cloudy summers and an increase in summer precipitation led to an overall positive water balance. The southerly shift of the jet stream due to glaciation in the Northern Hemisphere offers another explanation: moist Westerlies transported rain over the plateau and produced a positive water balance (Ön *et al*. 2018). These conditions are reflected in the pollen spectrum with an increase in Asteraceae and a decrease in Poaceae.

After the LGM, Landmann *et al*. (1996) and Litt *et al*. (2014) identified arid climatic conditions and associated falling lake levels at Lake Van. Facies 001B also indicates a falling lake level (between 128 and 120 cm b.l.b.) after the LGM at Lake Paravani. The spread of steppe vegetation is visible in the rise of Poaceae and Chenopodiaceae and a reduction in the already low share of arboreal pollen (Fig. 4).

In agreement with this, the absence of organic material at the base of cores PAR09-01 and PAR12-04 indicates arid climatic conditions around 12.5 cal. ka BP, which is consistent with the absence of organics in facies 001B. Following Messager *et al*. (2013), these arid climatic conditions persist until the Early Holocene. Joannin *et al*. (2014) also detected arid climatic conditions in the peat of the Zarishat bog in Armenia until *c*. 8200 cal. A BP.

Facies B9 in drill-core PAR09-01 represents the phase from 8355 to 1600 cal. BP. It is characterized by a remarkable increase in organic content and a decrease in detrital input, inferring wetter climatic conditions, increased productivity in the lake, and a spreading of vegetation in the Lake Paravani catchment (Messager *et al*. 2021). In contrast, such conditions cannot be inferred in drill-core ICE001 until facies 001C. A hiatus (H2) in facies 001B around 88 cm b.l.b. (below the palaeo-beach layer) is the best explanation for these differences; it fits with the identified sublittoral to littoral or fluvial conditions. Messager *et al*. (2021) also identified a hiatus at a depth of 69 cm in core PAR12-04, which they interpreted as evidence for a lower lake level around 2.8 cal. ka BP. The hiatus identified by Messager *et al*. (2021) matches our hiatus H1 both in terms of depth below lake bottom and the chronological classification (age at 72.5 cm b.l.b.: 3723–3559 cal. a BP, age at 66.5 cm b.l.b.: 2116–1405 cal. a BP) and therefore consolidates the conclusion of a complete emerging of the lake during that time.

An expansion of the Siberian High-Pressure Area and the associated blocking of the humid Westerlies during these times provides the climatic explanation. Joannin *et al*. (2014) proposed as well several arid phases, starting in the Middle Holocene; Simsek and Cagatay (2018) also reported arid climatic conditions and low lake levels of Lake Van during the period 3.5–1.4 cal. ka BP.

For the period from the beginning of the Late Holocene until the present, Messager *et al*. (2021) inferred high productivity in Lake Paravani and warmer temperatures in its catchment from organic-rich sediments. The sharp increase in the organic carbon content in facies 001C strongly supports these conclusions. Furthermore, a rising or constantly high lake level is inferred from the sediments of facies 001C. After about

2 cal. ka BP a climate regime similar to today's became established (Wick *et al*. 2003).

Archaeological implications of the new findings

The lake level minimum at 4.5 cal. ka BP and the corresponding palaeo-shoreline interpreted from the sediment cores, followed by a positive water balance and reforestation, have interesting implications for the archaeology of human occupation in Javakheti. The region has attracted humans for millennia, despite its high altitudes and contemporarily harsh climate, which has earned it the moniker of 'the Siberia of Georgia'. This attraction is perhaps best exemplified by the long-term exploitation of the abundant, high-quality, Chikiani obsidian source, located just northeast of Lake Paravani. Chikiani obsidian was made into obsidian tools used across a large part of the South Caucasus from the Palaeolithic at least until the Iron Age (Le Bourdonnec *et al*. 2012; Erb-Satullo *et al*. 2023). Exploitation of Chikiani obsidian, however, is only indirectly correlated with the kinds of human activities (e.g. permanent settlement, agricultural, and/or animal pasturing) that might produce impacts visible in palaeoenvironmental reconstructions.

Holocene traces of human occupation on the plateau itself are dated to the Mesolithic (beginning as early as 11 cal. ka BP), Neolithic (8–7 cal. ka BP) and Chalcolithic (7–6 cal. ka BP) but these phases of occupation have only recently begun to be defined (Varoutsikos *et al*. 2017). Recent surveys and excavations in Samtskhe, west of Javakheti, have brought Early Bronze Age occupations in southern Georgia into sharper focus, though these sites are somewhat lower (~1600 m a.s.l.) than much of the Javakheti Plateau (Kakhiani *et al*. 2013; Anderson *et al*. 2018). Early Bronze Age (*c*. 5.5–4.5 cal. ka BP) sites are known from Javakheti (Narimanishvili 2019: p. 67), including burials around Paravani (Kvavadze & Kakhiani 2010), but Early Bronze Age sites are less well documented than in other regions of Georgia. In this light, the comments of Messager *et al*. (2021) on Paravani showing little evidence of human impact during this period may indicate low overall levels of human occupation in the areas closest to Paravani, an observation that is generally consistent with our results. The concentrations of Cerealia and plantago-type pollen are so low that a statement on the expansion of agriculture would be tentative. However, it is worth noting that pollen evidence from contemporary burials found at altitudes of 2100–2300 m a.s.l. identified evidence of agriculture and apiculture in the products deposited in burials (Kvavadze *et al*. 2006; Kvavadze & Kakhiani 2010). This apparent contrast might be explained by the differing depositional process associated with a natural lake core vs. a constructed burial. Pollen from the latter is more likely to be a product of direct human action associated with the burial, and might include food products brought from lower altitudes.

By contrast, from the Late Bronze Age, there is good evidence of intensive, likely permanent human habitation in the area. More than 100 sites, from smaller fortified outposts to large multi-walled fortresses with associated settlements, are found across the Javakheti Plateau (Narimanishvili 2019). Few have been subjected to comprehensive excavation with radiocarbon dating, but surface materials and comparisons with similar sites on the Dmanisi and Trialeti plateaus (east and northeast of Javakheti) suggest that many originate in the Late Bronze and Early Iron Ages (1500–800 BC) (Narimanishvili 2012; Erb-Satullo & Jachvliani 2022). Perhaps most intriguing are the high-altitude fortresses at Abuli and Shaori (2600–2700 m a.s.l.), situated on scree-covered peaks well above the modern limit of agriculture and settlement (~2100 m a.s.l.). Given their elevated location, unusual character, and the absence of datable pottery, the chronology of these sites is more ambiguous than that of fortresses lower down on the plateau. A date in the 2nd millennium BC for their initial construction is conceivable, if unproven. Evidence for a more forested landscape and temperate climate during the Late Bronze and Early Iron Ages hints at more favourable conditions for these high-altitude sites, but it must be stressed that the nature of human activity there (e.g. temporary refuges, ritual sites, or permanent settlements) is very unclear. Therefore, the modest decline in arboreal pollen at this time is not necessarily caused by anthropogenic deforestation and expansion of agriculture.

Conclusions

Due to our analysis of sediment cores from the southern margin of Lake Paravani it is possible to reconstruct the landscape and vegetation history of the lake and its catchment for the Holocene and Late Pleistocene. Although the interpretation of the data remains challenging and fragmented due to several possible hiatuses, it is still possible to cover a time-span of almost the last 30 ka, thus extending the existing record beyond the LGM.

- Phase I (approx. 28–16 cal. ka BP). A glacially dominated landscape existed around Lake Paravani with sparse vegetation cover, poorly developed soils, and predominant physical weathering. Some uncertainties in the interpretation are due to the unclear influences of an ice cover on sedimentation.
- Phase II (approx. 16–6 cal. ka BP). The landscape and climatic conditions underlying these sedimentary facies are not easily deciphered. The shift of the facies to sublittoral conditions indicates a lowered lake level and an increase in aridity. Consistent with this, the absence of organic material is associated with cold temperatures and sparse steppe vegetation cover in

the catchment. The lack of dating and the possibility of hiatuses further complicate the interpretation and allow only a partial reconstruction of this period.

- Phase III (approx. 6–1 cal. ka BP). A low lake level was identified at approximately 4.5 cal. ka BP at the base of facies 001C, whereas the uppermost 60 cm b.l.b. of the core records a rising lake level. Hence, a positive water balance is inferred, which is associated with warmer temperatures and a humid climate (which is also indicated slightly earlier by Kvavadze and Kakhiani (2010)), which in turn are confirmed by the presence of organic carbon and increasing rates of chemical weathering intensity. Arboreal pollen content rises to almost 50% and indicates open mixed forests. Human settlements occur from the Bronze Age onwards in the region.

Based on these findings, we can confirm that high mountain lakes in general, and Lake Paravani in particular, are highly suitable and sensitive archives for palaeogeographical reconstructions. Our gained chronostratigraphy reflects trends of other high mountain lakes of the Caucasus region and from the Anatolian Plateau and extends our knowledge of landscape evolution beyond the Pleistocene–Holocene boundary and the LGM.

Acknowledgements. – This study was financially supported by the project 'High mountain large lakes as a key component of local environment, study of natural and man-made impacts' (Project # G-2153) by International Science and Technology Foundation and the Georgian National Science Foundation (SRNSF) (project number FR-18-22377). We thank the team of the Ilia State University for their support during the challenging fieldwork under severe winter conditions. Thanks to Stephan Opitz and Nicole Mantke for their support in the laboratory. Finally, we thank the anonymous reviewers for their constructive and encouraging advice and feedback. Open Access funding enabled and organized by Projekt DEAL.

Author contributions. – All authors made substantial contributions to this research and approved the final version of the manuscript. ME, HL, HB and DG conceived the study. LA, LN, ME, GK, DG, HB and HL performed the fieldwork. Laboratory analyses were conducted by DG, NU and LN and supervised by HL, ME, TK and HB. DG, HL, NE-S, WMvdM, TK, GK, HB and ME wrote the manuscript. All authors commented on the manuscript and approved the final version.

Data availability statement. – All data that are used will be made accessible via Zenodo or a comparable platform.

References

Akhalkatsi, M. 2009: *Conservation and Sustainable Use of Crop Wild Relatives in Samtskhe – Javakheti*. 165 pp. Georgian Society of Nature Explorers "Orchis", Tbilisi.

Anderson, W., Negus Cleary, M., Birkett-Rees, J., Krsmanovic, D. & Tskvitinidze, N. 2018: Gateway to the Yayla: the varneti archaeological complex in the Southern Caucasus highlands. *European Journal of Archaeology 22*, 22–43.

Arabuli, G., Kvavadze, E., Kikodze, D., Connor, S. E., Kvavadze, E., Bagaturia, N., Murvanidze, M. & Arabuli, T. 2008: The Krummholz beech woods of Mt. Tavkvetili (Javakheti plateau, Southern Georgia) – a relict ecosystem. *Proceedings of the Institute of Zoology 23*, 194–213.

Arnaud, F., Poulenard, J., Giguet-Covex, C., Wilhelm, B., Revillon, S., Jenny, J. P., Revel, M., Enters, D., Bajard, M., Fouinat, L., Doyen, E., Simonneau, A., Pignol, C., Chapron, E., Vannière, B. & Sabatier, P. 2016: Erosion under climate and human pressures: an alpine lake sediment perspective. *Quaternary Science Reviews 152*, 1–18.

Arnaud, F., Révillon, S., Debret, M., Revel, M., Chapron, E., Jacob, J., Giguet-Covex, C., Poulenard, J. & Magny, M. 2012: Lake Bourget regional erosion patterns reconstruction reveals Holocene NW European Alps soil evolution and paleohydrology. *Quaternary Science Reviews 51*, 81–92.

Björck, S. & Wohlfarth, B. 2001: Chronostratigraphic techniques in paleolimnology. *In* Last, W. M. & Smol, J. P. (eds.): *Tracking Environmental Change Using Lake Sediments. Volume 1: Basins Analysis, Coring and Chronological Techniques*, 204–245. Kluwer Academic Publishers, Dordrecht.

Blott, S. J. & Pye, K. 2001: GRADISTAT: a grain size distribution and statistics package for the analysis of unconsolidated sediments. *Earth Surface Processes and Landforms 26*, 1237–1248.

Bridge, J. S. & Demicco, R. V. 2008: *Earth Surface Processes, Landforms and Sediment Deposits*. 832 pp. Cambridge University Press, Cambridge.

Bronk Ramsey, C. 2008: Deposition models for chronological records. *Quaternary Science Reviews 27*, 42–60.

Bronk Ramsey, C. 2021: OxCal 4.4. 4 Calibration Program. Available at: https://c14.arch.ox.ac.uk/oxcal.html.

Cagatay, N. M., Ögretmen, N., Damci, E., Stockhecke, M., Sancar, Ü., Eris, K. K. & Özeren, S. 2014: Lake level and climate records of the last 90 ka from the Northern Basin of Lake Van, eastern Turkey. *Quaternary Science Reviews 104*, 97–116.

Catalan, J., Camarero, L., Felip, M., Pla, S., Ventura, M., Buchaca, T., Bartumeus, F., Mendoza, G., Miro, A., Casamayor, E. O., Medina-Sanchez, J. M., Bacardit, M., Altuna, M., Bartons, M. & Quijano, D. D. 2006: High mountain lakes: extreme habitats and witnesses of environmental changes. *Limnetica 25*, 551–584.

Catalan, J., Pla-Rabés, S., Wolfe, A. P., Smol, J. P., Rühland, K. M., Anderson, N. J., Kopáček, J., Stuchlík, E., Schmidt, R., Koinig, K. A., Camarero, L., Flower, R. J., Heiri, O., Kamenik, C., Korhola, A., Leavitt, P. R., Psenner, R. & Renberg, I. 2013: Global change revealed by palaeolimnological records from remote lakes: a review. *Journal of Paleolimnology 49*, 513–535.

Cohen, A. S. 2003: *Paleolimnology. The History and Evolution of Lake Systems*. 528 pp. Oxford University Press, New York.

Connor, S. E. & Kvavadze, E. V. 2009: Modelling late quaternary changes in plant distribution, vegetation and climate using pollen data from Georgia, Caucasus. *Journal of Biogeography 36* (3), 529–545.

Connor, S., Sagona, C. & Jamieson, A. 2020: Vegetation, Fire and Grazing Dynamics in Mtskheta, Georgia, and their implications for human economic strategies since 2000 BC. *Ancient Near Eastern Studies 57*, 149–188.

Connor, S. E., Thomas, I. & Kvavadze, E. 2007: A 5600-yr history of changing vegetation, sea levels and human impacts from the Black Sea coast of Georgia. *The Holocene 17*, 25–37.

Connor, S. E., Thomas, I., Kvavadze, E. V., Arabuli, G. J., Avakov, G. S. & Sagona, A. 2004: A survey of modern pollen and vegetation along an altitudinal transect in southern Georgia, Caucasus region. *Review of Palaeobotany and Palynology 129*, 229–250.

Cromartie, A., Blanchet, C., Barhoumi, C., Messager, E., Peyron, O., Ollivier, V., Sabatier, P., Etienne, D., Karakhanyar, A., Khatchadourian, L., Smith, A. T., Badalyan, R., Perello, B., Lindsay, I. & Joannin, S. 2020: The vegetation, climate, and fire history of a mountain steppe: a Holocene reconstruction from the South Caucasus, Shenkani, Armenia. *Quaternary Science Reviews 246*, 106485, https://doi.org/10.1016/j.quascirev.2020.106485.

Croudace, I. W., Rindby, A. & Rothwell, R. G. 2006: ITRAX: description and evaluation of a new multi-function X-ray core scanner. *Geological Society of London, Special Publication 267*, 51–63.

Dede, V., Cicek, I., Akif Sarikaya, M., Ciner, A. & Uncu, L. 2017: First cosmogenic geochronology from the Lesser Caucasus: Late Pleistocene glaciation and rock glacier development in the Karcal Valley, NE Turkey. *Quaternary Science Reviews 164*, 54–67.

Dusar, B., Verstraeten, G., Notebaert, B. & Bakker, J. 2011: Holocene environmental change and its impact on sediment dynamics in the Eastern Mediterranean. *Earth Science Reviews 108*, 137–157.

Erb-Satullo, N. L. & Jachvliani, D. 2022: Fortified communities in the South Caucasus: insights from Mtsvane Gora and Dmanisis Gora. *Journal of Field Archaeology 47*, 305–323.

Erb-Satullo, N. L., Rutter, M., Frahm, E., Jachvliani, D., Albert, P. G. & Smith, V. C. 2023: Obsidian exchange networks and highland-lowland interaction in the Lesser Caucasus borderlands. *Journal of Archaeological Science: Reports 49*, 103988, https://doi.org/10.1016/j.jasrep.2023.103988.

Eris, K. K., Ön, S. A., Cagatay, M. N., Ülgen, U. B., Ön, Z. B., Gürocak, Z., Arslan, T. N., Akkoca, D. B., Damci, E., Inceöz, M. & Okan, Ö. Ö. 2018: Late Pleistocene to Holocene paleoenvironmental evolution of Lake Hazar, Eastern Anatolia, Turkey. *Quaternary International 486*, 4–16.

Faegri, K. & Iversen, K. 1989: *Textbook of Pollen Analysis*. 328 pp. John Wiley and Sons, Chichester (reprint in 2000 by Blackburn Press, Caldwell, New Jersey).

Folk, R. L. & Ward, W. C. 1957: Brazos River Bar: a study in the significance of grain size parameters. *Journal of Sedimentary Petrology 27*, 3–26.

Fritz, M., Unkel, I., Lenz, J., Gajewski, K., Frenzel, P., Paquette, N., Lantuit, H., Körte, L. & Wetterich, S. 2018: Regional environmental changes versus local signal preservation in Holocene thermokarst lake sediments: a case study from Herschel Island, Yukon (Canada). *Journal of Paleolimnology 60*, 77–96.

Gee, G. W. & Or, D. 2002: Particle-size analysis. *In* Dane, J. H. & Topp, G. C. (eds.): *Methods of Soil Analysis. Part 4 – Physical Methods*, 255–293. Soil Science Society of America *Book Series 5*, Madison, Wisconsin.

van Geel, B. 2001: Non-pollen palynomorphs. *In* Smol, J. P., Birks, H. J. B. & Last, W. M. (eds.): *Tracking Environmental Change Using Lake Sediments: Terrestrial, Algal, and Siliceous Indicators 3*, 99–119. Kluwer Academic Publishers, Dordrecht.

Grimm, E. C. 1987: CONISS: a FORTRUN 77 program for stratigraphically constrained cluster analysis by the method of incremental sum of squares. *Computers and Geosciences 13*, 13–55.

Grimm, E. C. 1990: Tilia and Tilia Graph: PC spreadsheet and graphics software for pollen data. *INQUA, Working Group on Data-Handling Methods, Newsletter 4*, 5–7.

Guillou, H., Singer, B., Laj, C., Kissel, C., Scaillet, S. & Jicha, B. R. 2004: On the age of the Laschamp geomagnetic event. *Earth and Planetary Science Letters 227*, 331–343.

Hansen, S., Mirtskhulava, G. & Bastert-Lamprichs, K. 2007: Aruchlo: Neolithic settlement mound in the Caucasus. *Neo-Lithics 1/07*, 13–18.

Japoshvili, B. 2008: Long-term assessment of a vendace (*Coregonus albula* L.) stock in Lake Paravani, South Georgia. *Advances in Limnology 63*, 363–369.

Jijelava, B. & Simonia, I. 2016: Megalithic monument of Abuli, Georgia, and possible astronomical significance. *Indian Journal of Science and Technology 9*, 1–5, https://doi.org/10.17485/ijst/2016/v9i31/91741.

Joannin, S., Ali, A. A., Ollivier, V., Roiron, P., Peyron, O., Chevaux, S., Nahepetyan, S., Tozalakyan, P., Karakhanyan, A. & Chataigner, C. 2014: Vegetation, fire and climate history of the Lesser Caucasus: a new Holocene record from Zarishat fen (Armenia). *Journal of Quaternary Science 29*, 70–82.

Kakhiani, K., Sagona, A., Sagona, C., Kvavadze, E., Bedianashvili, G., Massager, E., Martin, L., Herrscher, E., Martkoplishvili, I., Birkett-Rees, J. & Longford, C. 2013: Archaeological investigations at Chobareti in southern Georgia, the Caucasus. *Ancient Near Eastern Studies 50*, 1–138.

Kaplan, G. 2013: Palynological analysis of the late Pleistocene terrace deposits of Lake Van, eastern Turkey: reconstruction of paleovegetation and paleoclimate. *Quaternary International 292*, 168–175.

Kleeberg, A., Freidank, A. & Jöhnk, K. 2013: Effects of ice cover on sediment resuspension and phosphorus entrainment in shallow lakes: combining in situ experiments and wind-wave modeling. *Limnology and Oceanography 58*, 1819–1833.

de Klerk, P., Haberl, A., Kaffke, A., Krebs, M., Matchutadze, I., Minke, M., Schulz, J. & Joosten, H. 2009: Vegetation history and environmental development since ca 6000 cal yr BP in and around Ispani 2 (Kolkheti lowlands, Georgia). *Quaternary Science Reviews 28*, 890–910.

Kvavadze, E., Gambashidze, I., Mindiashvili, G. & Gogochuri, G. 2006: The first find in southern Georgia of fossil honey from the Bronze Age, based on palynological data. *Vegetation History and Archaeobotany 16*, 399–404.

Kvavadze, E. & Kakhiani, K. 2010: Palynology of the Paravani burial mound (Early Bronze Age, Georgia). *Vegetation History and Archaeobotany 19*, 469–478.

Kvavadze, E., Sagona, A., Martkoplishvil, I., Chichinadze, M., Jalabadze, M. & Koridze, I. 2015: The hidden side of ritual: new palynological data from Early Bronze Age Georgia, the Southern Caucasus. *Journal of Archaeological Science 2*, 235–245.

Kylander, M. E., Ampel, L., Wohlfarth, B. & Veres, D. 2011: High-resolution X-ray fluorescence core scanning analysis of Les Echets (France) sedimentary sequences: new insights from chemical proxies. *Journal of Quaternary Science 26*, 109–117.

Laermanns, H., Elashvili, M., Kirkitadze, G., Loveluck, C. P., May, S. M., Kelterbaum, D., Papuashvili, R. & Brückner, H. 2024: The Bronze Age occupation of the Black Sea coast of Georgia – new insights from settlement mounds of the Colchian plain. *Geoarchaeology 39*, 335–350.

Laermanns, H., Kelterbaum, D., May, S. M., Elashvili, M., Opitz, S., Hülle, D., Rölkens, J., Verheul, J., Riedesel, S. & Brückner, H. 2018a: Mid- to Late Holocene landscape changes in the Rioni Delta area (Kolkheti lowlands, W Georgia). *Quaternary International 465*, 85–98.

Laermanns, H., Kirkitadze, G., May, S. M., Kelterbaum, D., Opitz, S., Heisterkamp, A., Basilaia, G., Elashvili, M. & Brückner, H. 2018b: Bronze Age settlement mounds on the Colchian plain at the Black Sea coast of Georgia – a geoarchaeological perspective. *Geoarchaeology 33*, 453–469.

Laermanns, H., May, S. M., Kelterbaum, D., Kirkitadze, G., Opitz, S., Navrozashvili, L., Elashvili, M. & Brückner, H. 2019: Coastal lowland and floodplain evolution along the lower reach of the Supsa River (Western Georgia). *E&G Quaternary Science Journal 68*, 119–139.

Landmann, G. & Reimer, A. 1996: Climatically induces lake level changes at Lake Van, Turkey, during the Pleistocene/Holocene transition. *Global Biogeochemical Cycles 10* (4), 797–808.

Le Bourdonnec, F.-X., Nomade, S., Poupeau, G., Guillou, H., Tushabramishvili, N., Moncel, M.-H., Pleurdeau, D., Agapishvili, T., Voinchet, P., Mgeladze, A. & Lordkipanidze, D. 2012: Multiple origins of Bondi Cave and Ortvale Klde (NW Georgia) obsidians and human mobility in Transcaucasia during the Middle and Upper Palaeolithic. *Journal of Archaeological Science 39*, 1317–1330.

Lebedev, V. A. 2015: *Geological (Volcanological) Map of Javakheti Volcanic Area (Lesser Caucasus). Edition of 2015-2. 1:200,000*. IGEM RAS, Moscow.

Lebedev, V. A., Budnov, S. N., Dudauri, O. Z. & Vashakidze, G. T. 2008: Geochronology of Pliocene Volcanism in the Dzhavakheti Highland (the Lesser Caucasus). Part 2: eastern part of the Dzhavakheti Highland. *Stratigraphy and Geological Correlation 16*, 553–574.

Leemann, A. & Niessen, F. 1994: Holocene glacial activity and climatic variations in the Swiss Alps: reconstructing a continuous record from proglacial lake sediments. *The Holocene 4*, 259–268.

Leroyer, C., Joannin, S., Aoustin, D., Ali, A. A., Peyron, O., Ollivier, V., Tozalakyan, P., Karakhanya, A. & Jude, F. 2016: Mid Holocene vegetation reconstruction from Vanevan peat (south-east shore of Lake Sevan, Armenia). *Quaternary International 395*, 5–18.

Litt, T., Pickarski, N., Heumann, G., Stockhecke, M. & Tzedakis, P. C. 2014: A 600,000-year long continental pollen record from Lake Van, eastern Anatolia (Turkey). *Quaternary Science Reviews 104*, 30–41.

Messager, E., Belmecheri, S., Von Grafenstein, U., Nomade, S., Ollivier, V., Voinchet, P., Puaud, S., Courtin-Nomade, A., Guillou, H., Mgeladze, A., Dumoulin, J.-P., Mazuy, A. & Lordkipanidze, D. 2013: Late Quaternary record of the vegetation and catchment-related changes from Lake Paravani (Javakheti, South Caucasus). *Quaternary Science Reviews 77*, 125–140.

Messager, E., Lebreton, V., Marquer, L., Russo-Ermolli, E., Orain, R., Renault-Miskovsky, J., Lordkipanidze, D., Despriee, J., Peretto, C. & Arzarello, M. 2011: Palaeoenvironments of early hominins in temperate and Mediterranean Eurasia: new palaeobotanical data from Palaeolithic key-sites and synchronous natural sequences. *Quaternary Science Reviews 30*, 1439–1447.

Messager, E., Lordkipanidze, D., Kvavadze, E., Ferring, C. R. & Voinchet, P. 2009: Palaeoenvironmental reconstruction of Dmanisi site (Georgia) based on palaeobotanical data. *Quaternary International 223–224*, 20–27.

Messager, E., Poulenard, J., Sabatier, P., Develle, A.-L., Wilhelm, B., Nomade, S., Scao, V., Giguet-Covex, C., Von Grafenstein, U., Arnaud, F., Malet, E., Mgeladze, A., Herrscher, E., Banhan, M., Mazuy, A., Dumoulin, J.-P., Belmecheri, S. & Lordkipanidze, D. 2021: Paravani, a puzzling lake in the South Caucasus. *Quaternary International 579*, 6–18.

Meyers, P. A. & Teranes, J. L. 2002: Sediment organic matter. *In* Last, W. M. & Smol, J. P. (eds.): *Tracking Environmental Change Using Lake Sediments. Volume 2: Developments in Paleoenvironmental Research*, 239–269. Kluwer Academic Publishers, Dordrecht.

Moore, P. D., Webb, J. A. & Collinson, M. E. 1991: *Pollen Analysis*. 216 pp. Blackwell Scientific Publication, Oxford.

Moser, K. A., Baron, J. S., Brahney, J., Oleksy, I. A., Saros, J. E., Hundey, E. J., Kopáček, J. H., Sommaruga, R. I., Kainz, M. J. J., Strecker, A. L. K., Chandra, S. L., Walters, D. M. M., Preston, D. L. N., Michelutti, N. O., Lepori, F. P., Spaulding, S. A. Q., Christianson, K. R. R., Melack, J. M. & Smol, J. P. 2019: Mountain lakes: eyes on global environmental change. *Global and Planetary Change 178*, 77–95.

Narimanishvili, G. 2012: Archaeological investigations in Trialeti. *In* Avetisyan, P. S. & Bobokhyan, A. (eds.): *Archaeology of Armenia in Regional Context: Proceedings of the International Conference Dedicated to the 50th Anniversary of the Institute of Archaeology and Ethnography, held on September 15th-17th, 2009, Yerevan*, 88–105. Gitutyun, Yerevan.

Narimanishvili, D. 2019: *Sakartvelos Tsik'lop'uri Simagreebi/Cyclopean Fortresses in Georgia*. 493 pp. Shota Rustaveli National Science Foundation and the Georgian National Museum, Tbilisi (in Georgian).

Nomade, J., Chapron, E., Desmet, M., Reyss, J. L., Arnaud, F. & Lignier, V. 2005: Reconstructing historical seismicity from lake sediments (Lake Laffrey, Western Alps, France). *Terra Nova 17*, 350–357.

Nomade, S., Scao, V., Guillou, H., Messager, E., Mgeladze, A., Voinchet, P., Renne, P. R., Courtin-Nomade, A., Bardintzeff, J. M., Ferring, R. & Lordkipanidze, D. 2016: New $^{40}Ar/^{39}Ar$, unspiked K/Ar and geochemical constrains on the Pleistocene magmatism of the Samtskhe-Javakhet highlands (Republic of Georgia). *Quaternary International 395*, 45–59.

Nutz, A., Schuster, M., Ghienne, J.-F., Roquin, C. & Bouchette, F. 2018: Wind-driven waterbodies: a new category of lake within an alternative sedimentologically-based lake classification. *Journal of Paleolimnology 59*, 189–199.

Okrostsvaridze, A., Popkhadze, N., Bluashvili, D., Chang, Y. H. & Skhirtladze, I. 2016: Pliocene-Quaternary Samtskhe-Javakheti Volcanic Highland, Lesser Caucasus – as a result of mantle plumes activity. *IGCP 610 Fourth Plenary Meeting and Field Trip, 02.10–09.10.2016*, 1–3. Tbilisi, Georgia.

Ön, Z. B., Akcer-Ön, S., Özeren, M. S., Eris, K. K., Greaves, A. M. & Cagatay, M. N. 2018: Climate proxies for the last 17.3 ka from Lake Hazar (eastern Anatolia), extracted by independent component analysis of μ-XRF data. *Quaternary International 486*, 17–28.

Pasquare, F. A., Tormey, D., Vezzoli, L., Okrostsvaridze, A. & Tutberidze, B. 2011: Mitigating the consequences of extreme events on strategic facilities: evaluation of volcanic and seismic risk affecting the Caspian oil and gas pipelines in the Republic of Georgia. *Journal of Environmental Management 92*, 1774–1782.

Ramsey, C. B. & Lee, S. 2013: Recent and planned developments of the program OxCal. *Radiocarbon 55*, 720–730.

Rebai, S., Philip, H., Dorbath, L., Borisoff, B., Haessler, H. & Cisternas, A. 1993: Active tectonics in the Lesser Caucasus: coexistence of compressive and extensional structures. *Tectonics 12*, 1089–1114.

Reille, M. 1992: *Pollen et spores d'Europe et d'Afrique du Nord*. 543 pp. Laboratoire de Botanique historique et Palynologie, Marseille, France.

Reimer, P. J., Austin, W. E., Bard, E., Bayliss, A., Blackwell, P. G., Ramsey, C. B., Butzin, M., Cheng, H., Edwards, R. L. & Friedrich, M. 2020: The IntCal20 Northern Hemisphere radiocarbon age calibration curve (0–55 cal kBP). *Radiocarbon 62*, 725–757.

Robles, M., Peyron, O., Brugiapaglia, E., Menot, G., Dugerdil, L., Ollivier, V., Ansanay-Alex, S., Develle, A.-L., Tozalakyan, P., Meliksetian, K., Sahakyan, K., Sahakyan, L., Perello, B., Badalyan, R., Colombie, C. & Joannin, S. 2022: Impact of climate changes on vegetation and human societies during the Holocene in the South Caucasus (Vanevan, Armenia): a multiproxy approach including pollen, NPPs and brGDGTs. *Quaternary Science Reviews 277*, 107297, https://doi.org/10.1016/j.quascirev.2021.107297.

Rothwell, R. G. & Croudace, I. W. 2015: Micro-XRF studies of sediment cores. A perspective on capability and application in the environmental sciences. *In* Rothwell, R. G. & Croudace, I. W. (eds.): *Micro-XRF Studies of Sediment Cores*, 25–102. Springer, Heidelberg.

Schnurrenberger, D., Russel, J. & Kelts, K. 2003: Classification of lacustrine sediments based on sedimentary components. *Journal of Paleolimnology 29*, 141–154.

Sharkov, E., Lebedev, V., Chugaev, A., Zabarinskaya, L., Rodnikov, A. & Sergeeva, N. 2015: The Caucasian-Arabian segment of the Alpine-Himalayan collisional belt: geology, volcanism and neotectonics. *Geoscience Frontiers 6*, 513–522.

Shatilova, I., Rukhadze, L. & Mchedlishvili, N. 2010: The stages of development of vegetation climate of Western Georgia during the Middle and Late Pleistocene. *Proceedings of the Natural and Prehistoric Section (Georgian National Museum) 2*, 75–81.

Shebalin, N. V. & Tatevossian, R. E. 1997: Catalogue of large historical earthquakes of the Caucasus. *In* Giardiniand, D. & Balassanian, S. (eds.): *Historical and Prehistorical Earthquakes in the Caucasus. NATO ASI Series 2*, 201–232. Kluwer Academic Publishers, Dordrecht.

Simsek, F. B. & Cagatay, M. N. 2018: Late Holocene high-resolution multi-proxy climate and environmental records from Lake Van, eastern Turkey. *Quaternary International 486*, 57–72.

Stevens, L. R., Djamali, M., Andrieu-Ponel, V. & de Beaulieu, J.-L. 2012: Hydroclimatic variations over the past two glacial/interglacial cycles at Lake Urmia, Iran. *Journal of Paleolimnology 47*, 645–660.

Stock, F., Laermanns, H., Pint, A., Knipping, M., Wulf, S., Hassl, A., Heiss, A., Ladstaetter, S., Opitz, S., Schwaiger, H. & Brückner, H. 2020: Human-environment interaction in the hinterland of Ephesos. *Quaternary Science Reviews 244*, 106418, https://doi.org/10.1016/j.quascirev.2020.106418.

Stockhecke, M., Sturm, M., Brunner, I., Schmincke, H. U., Sumita, M., Kipfers, R., Cukur, D., Kwiecien, O. & Anselmetti, F. S. 2014: Sedimentary evolution and environmental history of Lake Van (Turkey) over the past 600 000 years. *Sedimentology 61*, 1830–1861.

Stockmarr, J. 1971: Tablets with spores used in absolute pollen analysis. *Pollen et Spores 13*, 615–621.

Strunk, A., Olsen, J., Sanei, H. & Rudra, A. 2020: Improving the reliability of bulk sediment radiocarbon dating. *Quaternary Science Reviews 242*, 106442, https://doi.org/10.1016/j.quascirev.2020.106442.

Stuiver, M., Reimer, P. J. & Reimer, R. W. 2021: CALIB 8.2. Available at: http://calib.org (accessed 07.02.2023).

von Suchodoletz, H., Kirkitadze, G., Koff, T., Fischer, M. L., Poch, R. M., Khosravichenar, A., Schneider, B., Glaser, B., Lindauer, S., Hoth, S., Skokan, A., Navrozashvili, L., Lobjanidze, M., Akhalaia, M., Losaberidze, L. & Elashvili, M. 2022: Human-environmental interactions and seismic activity in a late Bronze to Early Iron Age settlement center in the southeastern Caucasus. *Frontiers in Earth Science 10*, 964188, https://doi.org/10.3389/feart.2022.964188.

von Suchodoletz, H., Menz, M., Kühn, P., Sukhishvili, L. & Faust, D. 2015: Fluvial sediments of the Algeti River in southeastern Georgia – an archive of Late Quaternary landscape activity and stability in the Transcaucasian region. *Catena 130*, 95–107.

Varoutsikos, B., Mgeladze, A., Chahoud, J., Gabunia, M., Agapishvili, T., Martin, L. & Chataigner, C. 2017: From the Mesolithic to the Chalcolithic in the South Caucasus: new data from the Bavra Ablari rock shelter. *In* Batmaz, A., Bedianashvili, G. & Michalewicz, A. (eds.): *Context and Connection: Essays on the Archaeology of the Ancient near East in Honour of Antonio Sagona*, 233–255. Peeters Publishers, Leuven.

Vogel, J. S., Briskin, M., Nelson, D. E. & Southon, J. R. 1989: Ultra-small carbon samples and the dating of sediments. *Radiocarbon 31*, 601–609.

Wick, L., Lemcke, G. & Sturm, M. 2003: Evidence of Lateglacial and Holocene climatic change and human impact in eastern Anatolia: high-resolution pollen, charcoal, isotopic and geochemical records from the laminated sediments of Lake Van, Turkey. *The Holocene 13*, 665–675.

Yang, H., Ren, W., Cuz, Q.-Y. & Li, Q. 2021: Paleoclimatic indication of X-ray fluorescence core-scanned Rb/Sr ratios: a case study in the Zoige Basin in the eastern Tibetan Plateau. *Science China Earth Sciences 64*, 80–95.

Zolitschka, B., Behre, K.-B. & Schneider, J. 2003: Human and climatic impact on the environment as derived from colluvial, fluvial and lacustrine archives – examples from the Bronze Age to the Migration period, Germany. *Quaternary Science Reviews 22*, 81–100.

Supporting Information

Additional Supporting Information to this article is available at http://www.boreas.dk.

Fig. S1. Hydrological map of the catchments surrounding Lake Paravani and the Samsari range (following Lebedev 2015). Hydro modelling, using the ArcMap Hydrotools extension was applied. A consistent numerical hydro model was constructed, based on ALOS/SRTM 30-m resolution DEM, corresponding to a topographic base map of 1:50 000 scale. Beside the existing rivers more extended dried out water channels were found and are marked here with dashed lines (marked with dashed lines).

Fig. S2. Drilling from the lake's ice cover during fieldwork using a percussion corer (photo: Kirkitadze 2019).

Fig. S3. Transect of the retrieved sediment cores based on granulometry and measurement of magnetic susceptibility (black line) with a MS2K Bartington Magnetic susceptibility meter at 0.4-cm intervals.